The Journal of Experimental Biology 213, 63-71
Published by The Company of Biologists 2010
doi:10.1242/jeb.031708

In-line motion causes high thrust and efficiency in flapping foils that use power downstroke

S. C. Licht, M. S. Wibawa, F. S. Hover and M. S. Triantafyllou*
Department of Mechanical Engineering, Massachusetts Institute of Technology, Cambridge, MA 02139, USA
*Author for correspondence (mistetri@mit.edu)

Accepted 16 September 2009

SUMMARY

We show experimentally that flapping foil kinematics consisting of a power downstroke and a feathering upstroke together with a properly timed in-line motion, similar to those employed in forelimb propulsion of sea turtles, can produce high thrust and be hydrodynamically as efficient as symmetrically flapping foils. The crucial parameter for such asymmetrically flapping foils is a properly sized and timed in-line motion, whose effect is quantified by a new parameter, the advance angle, defined as the angle of the foil trajectory with respect to the horizontal, evaluated at the middle of the power downstroke. We show, in particular, that optimal efficiency in high aspect ratio rigid foils, accompanied by significant thrust production, is obtained for Strouhal numbers in the range 0.2–0.6 for Reynolds number equal to 13,000, and for values of the advance angle around 0.55π (100 deg.). The optimized kinematics consist of the foil moving back axially during the downstroke, in the direction of the oncoming flow, and rotating with a large pitch angle. This causes the force vector to rotate and become nearly parallel to the steady flow, thus providing a large thrust and a smaller transverse force. During the upstroke, the foil is feathering while it moves axially forward, i.e. away from the vorticity shed during the power stroke; as a result, the transverse force remains relatively small and no large drag force is produced. Observations from turtles confirm qualitatively the findings from the foil experiments.

Key words: flapping foil, asymmetric motion, in-line motion.

INTRODUCTION

The inspiration to study and use flapping foils for propulsion and maneuvering comes from animal observations. Insects and birds must employ non-symmetrical wing kinematics in order to provide a mean lift to support their weight, in addition to propulsive thrust (Ellington, 1999; Dickinson et al., 1999); however, even certain nearly neutrally buoyant swimming animals, which do not need significant mean lift forces, still employ non-symmetrical flapping, for reasons unrelated to hydrodynamics. Turtles, for example, employ a power downstroke that produces substantial thrust, followed by a feathering upstroke when very little thrust is produced. We address in this paper the following questions.

(1) What degradation in thrust production and efficiency results from the limitation to power the downstroke only?
(2) Which procedures optimize thrust production and efficiency?
(3) How do animals reduce unbalanced mean lift forces?

The thrust production of oscillating foils has been studied extensively numerically and experimentally because of its importance to the understanding of animal locomotion and for importing biomimetic principles to engineering (Koochesfahani, 1989; Anderson et al., 1998; von Ellenrieder et al., 2003; Triantafyllou et al., 2005; Blondeaux et al., 2005; Techet et al., 2005; Dong et al., 2006; Buchholtz and Smits, 2006; Buchholtz and Smits, 2008; Shyy and Liu, 2007).

For underwater locomotion of nearly neutrally buoyant animals, a steady lift force is not required; hence most studies have focused on foils which are flapping symmetrically either about a zero mean position or around a steady bias position, i.e. involving motion with symmetric upstroke and downstroke motions. Also, the majority of engineering studies consider foils free to move only transversely with respect to a steady incoming flow (Hover et al., 2004; Licht et al., 2004), because the number of kinematic parameters is reduced, resulting in easier implementation and with fewer mechanical parts; however, this restriction does not accurately reflect biological examples of high aspect ratio flapping propulsion, as shown in observational studies of steady swimming in birds (Lovvorn, 2001), reptiles (Davenport et al., 1984), mammals (Videler and Kamermans, 1985) and fish (Blake, 1980; Blake, 2004; Walker and Westneat, 1997; Lauder and Jayne, 1996). Ramamurti and colleagues (Ramamurti et al., 2002), Lauder and colleagues (Lauder et al., 2006), and Suzuki and Kato (Suzuki and Kato, 2008), among others, considered three-dimensional pivoted motion of a rigid or flexible fin in the shape of a fish pectoral fin.

Sea turtles demonstrate that body flexibility is not essential to achieve high maneuverability and good motion control when using flapping, high aspect ratio foils, and serve as a powerful inspiration for the design of underwater vehicles. As observed by Davenport (Davenport et al., 1984) and Wyneken (Wyneken, 1988), the forelimb kinematics of sea turtles in steady forward swimming are highly asymmetric and involve significant in-line motion: the upstroke can take twice as long as the downstroke to complete, and there is also significant limb motion in-line with the swimming direction, as the forelimbs are pulled back along the body during the downstroke, and pushed forward against the flow during the upstroke.

Sea turtle morphology is such that the forelimbs can produce much more torque in the downstroke than in the upstroke: juvenile turtles are barely capable of raising their limbs out horizontally from the shoulder when held in air (Davenport et al., 1984). Steady swimming in turtles typically consists of a powered, high angle of attack downstroke generating forward thrust and maneuvering forces, followed by a feathered upstroke, as noted by Wyneken

(Wyneken, 1988). Direct observation of turtles at the New England Aquarium with the goal of biomimetically assisting in the design of an underwater vehicle equipped with flapping foils, 'Finnegan the RoboTurtle' (Wolfe et al., 2006; Licht et al., 2004), also show that there can be a significant anterior–posterior motion of high aspect ratio oscillating foils during transient maneuvering behaviors.

Irrespective of the reasons why animals employ an asymmetric flapping pattern, the major questions are whether this asymmetry is detrimental to efficiency, how significant this reduction is if optimized kinematics are used, and how it is possible to design the asymmetric motion to avoid large steady lift forces. Herein we answer all three questions by testing experimentally a high aspect ratio foil, towed at steady speed and capable of arbitrary transverse and in-line oscillatory motion as well as rotation about its long axis.

MATERIALS AND METHODS

Experimental apparatus

We designed an experimental apparatus capable of: (i) imposing a steady motion to the overall apparatus along a specially designed tank with dimensions 2.4 m×0.75 m×0.75 m; (ii) rotating a vertically oriented foil about its spanwise axis (pitch motion); and (iii) imposing two degree of freedom motion in the horizontal plane; we will call the motion parallel to the steady translation of the apparatus 'in-line motion' and the motion perpendicular to the steady translation 'transverse motion'.

Hence, a large aspect ratio foil was towed steadily along the long axis of a water tank, while two linear motors imposed a horizontal planar motion, and a third motor imposed a rotation about the vertical axis, as depicted in Fig. 1. The foil was attached to the pitch motor at the one-third chord point, measured from the leading edge. Previous experiments with the apparatus had confirmed that over the speed range tested wave making resistance is negligible.

The foil position is fully described relative to the steadily moving frame of the platform with velocity U by the co-ordinates (x, y, θ), where the y direction is perpendicular to the incoming flow and perpendicular to the foil rotational axis. The positive x direction is parallel to the direction of steady motion of the foil (or parallel and opposite in direction to the equivalent oncoming steady flow). The pitch angle, θ, is the rotation about the vertical axis, where θ=0 when the foil chord is parallel to the equivalent incoming flow, with the leading edge oriented into the flow (Fig. 2). As shown in Fig. 3, on top of the steadily mounted platform there is a linear bearing allowing transient transverse motion; and on top of it another linear bearing allowing in-line transient motion. Two linear motors drive the transverse and in-line motions.

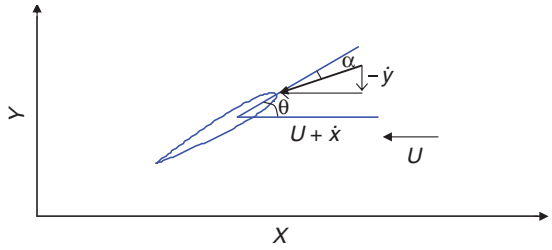

Fig. 2. Definition of motion parameters and nominal angle of attack (α) in the foil experimental apparatus. $\dot{x}$ denotes the foil in-line velocity; $-\dot{y}$ denotes the foil transverse velocity.

The foil used for this study was an extruded aluminium, NACA-0012 foil with a constant chord of 6.93 cm. The foil was clamped at one end to the shaft of a small servo-motor, with the axis of rotation at a distance of one-third of the chord length behind the leading edge. The foil pierced the free surface of the water and extended 0.53 m below the surface, where it terminated with a square end; the aspect ratio of the submerged part of the foil is 7.6, although the effective aspect ratio is higher because of the presence of the free surface and the proximity to the tank bottom.

The foil-bearing structure was mounted to the load side of a 6-axis load cell from JR3, Inc. (Woodland, CA, USA), with a linear load capacity of 110 N and moment capacity of 220 N m. The base of the force sensor was attached to the end of a cantilever beam, which was driven in the horizontal plane by a pair of linear servo-motors with 0.18 m travel. Amplified sensor output was differentially captured at 1 kHz with a National Instruments USB-6211 DAQ card (Austin, TX, USA). The foil drive motors were mounted to a rolling platform above the glass water tank.

Methodology

Although the foil was towed in the vertical position, we will still employ the term 'pitch motion' to describe the rotation of the foil about its axis, and the terms 'downstroke' to describe the portion of

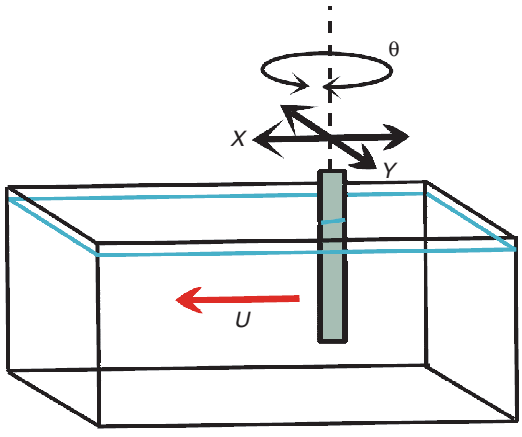

Fig. 1. Schematic diagram of foil experimental apparatus indicating direction of positive transverse, in-line and twist motion with respect to direction of steady translation. U, velocity; θ, pitch angle.

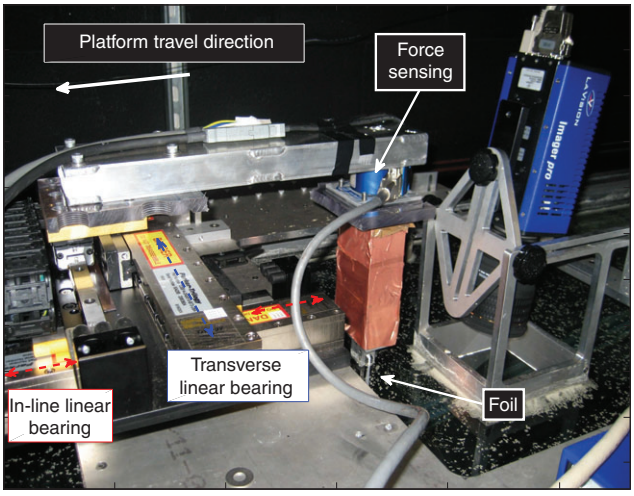

Fig. 3. View of single foil experimental apparatus showing actuators, sensor and foils mounted onto a moving platform.

the foil trajectory during which high power is expended, and 'upstroke' for the remaining, lower power part of the trajectory. An axial motion against the oncoming flow will be called 'upstream motion', and an opposite axial motion will be called 'downstream motion'.

To test our basic hypothesis on the effect of asymmetric flapping motion on thrust production and propulsive efficiency, asymmetry between upstroke and downstroke must be introduced parametrically to allow a systematic search and optimization. Hence, the parameters usually employed in symmetrically moving foils need to be carefully re-defined to accommodate asymmetry and allow an additional in-line motion, while remaining close to their original meaning.

First, each cycle of the foil motion was divided into two parts, a downstroke and an upstroke. The downstroke consists of the motion of the foil from the point of absolute maximum ($+y$) in the transverse excursion to the next absolute minimum ($-y$); the upstroke is the remaining part in the cycle. We define four new parameters to quantify the stroke asymmetries.

(1) Amplitude ratio, $A_{X/Y}=A_X/A_Y$, equal to the ratio of the in-line amplitude in m, A_X, and the transverse amplitude in m, A_Y, of the foil, where the excursions are measured relative to the steadily moving frame. We find the amplitude A_Y as one-half of the peak-to-peak transverse motion, and A_X as one-half of the peak-to-peak in-line motion; both motions relative to an observer moving with the steady speed of the foil, U. We allow A_X to take either positive values, which is analogous to the pulling horizontally and backward of a turtle's forelimb during a downstroke, or negative values if the opposite motion occurs. The transverse amplitude is always positive.

(2) Duration ratio $T_{U/D}=T_U/T_D$, equal to the ratio of the upstroke duration, T_U, over the downstroke duration, T_D, both in s. Increasing values of this ratio indicate a faster downstroke followed by a slower upstroke, typical of turtle locomotion.

(3) The upstroke and dowstroke angles of attack, $\alpha_{max,U}$ and $\alpha_{max,D}$, respectively. The maximum nominal angle of attack employed in symmetrically moving foils must be replaced with two parameters, the maximum angle of attack of the foil during the upstroke, and the maximum angle of attack of the foil during the downstroke.

Next, we define the Strouhal number as $St=2A_Yf/U$ (where f is the frequency in Hz), which has been found to influence significantly the efficiency of flapping foils; swimming and flying animals employ Strouhal numbers within a narrow range (Triantafyllou et al., 1991; Taylor et al., 2003; Rohr and Fish, 2004). The Strouhal number is a wake parameter, and must be based on the estimated width of the wake; hence we use the same definition as for a transversely heaving foil, since the best estimate for the wake width is the transverse peak-to-peak motion, i.e. $2A_Y$. Also, the average speed U is used, although the instantaneous speed between foil and water is modulated due to the introduction of a potentially significant in-line motion. As a result, one may expect differences in the specific values of the optimal Strouhal number in the present case relative to a purely transversely moving foil. As a result, we widened the range of St we investigated, to [0.2, 0.6].

We define also an additional parameter, which can be derived on the basis of the five parameters above, the 'advance angle', denoted as θ_{ADV}. This parameter can be derived from the basic parameters and depends critically on $A_{X/Y}$, $T_{U/D}$ and St; its significance is that it makes clear the effect of in-line motion on the overall foil kinematics. The advance angle is defined to be the angle of the foil trajectory with respect to the horizontal at the middle of the downstroke (power stroke). The trajectory is defined relative to a motionless observer (i.e. relative to the quiescent fluid of the tank). When the amplitude of in-line motion, A_X, is zero, the advance angle has the minimum possible value for the given kinematics; increasing A_X increases the advance angle, which may exceed 90 deg., i.e. the foil may appear to move backwards in the horizontal direction when at the middle of the power stroke. When the advance angle is 90 deg., the horizontal velocity of the foil with respect to the fluid is zero at the midpoint of the downstroke. Two examples of the resulting motion due to the variation in θ_{ADV} from 70 to 100 deg. are shown in Figs 4 and 5.

Parametric choices

Because of the large parametric space to be explored, we kept four parameters constant:

$$\alpha_{max,U} = 0 \text{ deg.},$$

$$\alpha_{max,D} = 40 \text{ deg.},$$

$$h_0 / c = A_Y / c = 0.9$$

and

$$T_U / T_D = 1,$$

where, h_0 is the amplitude of heave motion and c is chord length. The choices were designed to focus on the potential to improve thrust production through the introduction of in-line motion, given the restriction on the actuator power, which is available primarily, or even exclusively, during the downstroke. The downstroke angle of attack, $\alpha_{max,D}$, of 40 deg. has been shown to be effective in producing high thrust (albeit with relatively small hydrodynamic efficiency) in symmetrically pitching and heaving foils (Read et al., 2003). The upstroke angle of attack, $\alpha_{max,U}$, is set to zero to minimize

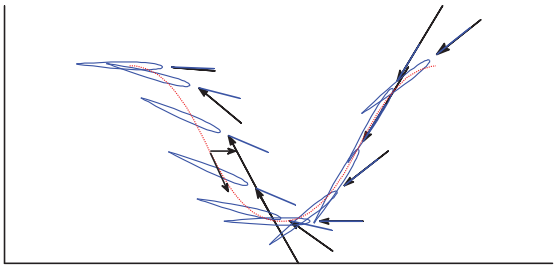

Fig. 4. Foil position with respect to fluid at regular intervals, when the advance angle $\theta_{ADV}=0.385\pi$. Arrows represent relative flow velocity. The nominal angle of attack is shown as the angle between the relative flow and the centerline of the foil.

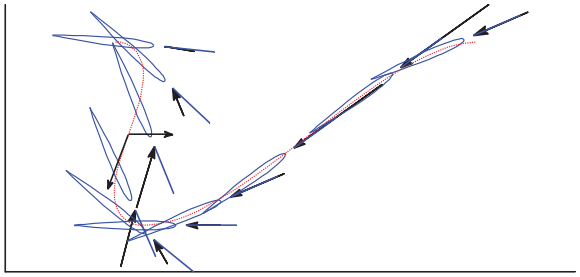

Fig. 5. Foil position with respect to fluid at regular intervals, when the advance angle $\theta_{ADV}=0.55\pi$. Arrows represent relative flow velocity. The nominal angle of attack is shown as the angle between the relative flow and the centerline of the foil.

upstroke power, and hence emulate a completely feathered recovery stroke. Transverse motion amplitude was selected to be of the order of one foil chord, which provides good performance in symmetrically flapping foils.

The following two parameters were varied systematically: St, through variation in frequency $f=1/(T_D+T_U)$, and θ_{ADV}, through variation in in-line amplitude A_X.

The Strouhal number St ranged in the interval [0.2, 0.6] in increments of 0.1. The advance angle θ_{ADV} was varied by increments of 0.055π (10 deg.), starting from the minimum possible value for each value of the Strouhal number St (i.e. starting with motion $A_X=0$), and ending in the maximum angle allowed by the apparatus.

Iterative procedure to obtain the kinematics

For each combination of these two parameters, St and θ_{ADV}, and given the values of the remaining parameters as outlined above, the following iterative numerical procedure was followed to determine: (a) the pitch angle $\theta(t)$, (b) the transverse motion $y(t)$, and (c) the in-line position $x(t)$, which would also result in: sinusoidal angle of attack profiles for both the first half (upstroke) and the second half (downstroke) of each cycle; obtaining the selected amplitudes on both the upstroke and the downstroke; and obtaining the selected value of θ_{ADV}.

The shape of $x(t)$ and $y(t)$ was selected to obtain a sinusoidal angle of attack, because earlier work on symmetrically flapping foils has shown that a sinusoidal variation of the angle of attack is very effective in producing high thrust and high hydrodynamic efficiency (Hover et al., 2004; Read et al., 2003).

The procedure to determine the foil kinematics given the desired Strouhal number St, angle of advance θ_{ADV}, and maximum angle of attack α_0^D, and for given experimental values of the frequency f and velocity U, must be iterative because the motion $y(t)$ is not sinusoidal when the angle of attack and pitch angle are sinusoidal. On the basis of the defined parameters above, we can find the desired transverse amplitude (peak to peak) $A_{Ypp}=StU/f$; then the iterative procedure is as follows.

First, we assume a value of the ratio of in-line to transverse motion, $A_{X/Y}$ and we set the $x(t)$ and $y(t)$ motions to be in phase:

$$x(t) = A_{X/Y}\, y\,(t)$$

$$\dot{x}(t) = A_{X/Y}\, \dot{y}\,(t)\,, \qquad (1)$$

where $\dot{y}(t)$ is the time derivative of $y(t)$ (transverse velocity), and $\dot{x}(t)$ is the time derivative of $x(t)$ (in-line velocity). Note that $y(t)$ [and hence $x(t)$] is at this point an unknown function of t.

Next, we set the pitch angle, $\theta(t)$, and angle of attack, $\alpha(t)$, to be piecewise sinusoidal, i.e. consisting of a sinusoid in the upstroke and then a different sinusoid in the downstroke. For the downstroke:

$$\alpha(t) = \alpha_0^D \sin(\omega t)$$

$$\theta(t) = \theta_0^D \sin(\omega t)\,, \qquad (2)$$

where ω is the frequency of oscillation in rad s^{-1}. It must be noted that for given value of α_0^D and advance angle, θ_{ADV}, we calculate directly θ_0^D from the geometry at the midpoint of the downstroke:

$$\theta_0^D = \alpha_0^D - \theta_{ADV}\,. \qquad (3)$$

Hence, we have fully defined $\alpha(t)$ and $\theta(t)$ for the downstroke, using Eqns 2 and 3. Next we find the expression for the angle of attack:

$$\alpha(t) = -\arctan\left(\frac{\dot{y}(t)}{U+\dot{x}(t)}\right) + \theta(t)\,. \qquad (4)$$

Using Eqn 1, we can now solve Eqn 4 in terms of the unknown $\dot{y}(t)$, and hence find $\dot{x}(t)$ as well:

$$\dot{y}(t) = \frac{U\tan(\theta(t)-\alpha(t))}{1+A_{X/Y}\tan(\theta(t)-\alpha(t))}\,. \qquad (5)$$

Now we can calculate the total transverse excursion of the foil during the downstroke:

$$\Delta y_D = \int_0^{\frac{T}{2}} \dot{y}\,dt\,, \qquad (6)$$

and we iterate on the assumed value of $A_{X/Y}$ until the calculated value of Δy_D is sufficiently close to the desired value of A_{Ypp}, as dictated by the Strouhal number.

Once the downstroke paramaters are defined, we proceed to the upstroke, where the angle of attack $\alpha(t)$ and pitch angle $\theta(t)$ are also sinusoidal, but now the value of $A_{X/Y}$ required to recover from the downstroke is fixed, while θ_0^U is no longer constrained by θ_{ADV}. Hence, the variable θ_0^U is varied and the same procedure as above is followed, until the total excursion of the foil over the upstroke:

$$\Delta y_U = f(\theta_0^U) \qquad (7)$$

satisfies $\Delta y_U=\Delta y_D$.

Overall, then, we obtain a piecewise sinusoidal angle of attack for the given maximum angle of attack α_{max}, transverse amplitude and advance angle, achieved through the combination of a piecewise sinusoidal pitch angle and the calculated transverse and in-line motion.

The Reynolds number of the experiments was close to 13,000, based on a foil chord length of $c=6.93$ cm and for the steady towing speed of 0.2 m s^{-1}.

RESULTS

As a basis of comparison (control case), we measured first the forces on a symmetrically moving foil and for similar parametric values to those for the asymmetric tests, with the obvious exception of the upstroke angle of attack, which was set equal to the downstroke value, $\alpha_{max,U}=\alpha_{max,D}=40$ deg. Fig. 6 provides the thrust and lift coefficients (C_T and C_L, respectively) for the symmetrically moving foil for a complete cycle of motion. Error bars provide the estimate of the experimental error in the measurements. Symmetric forces

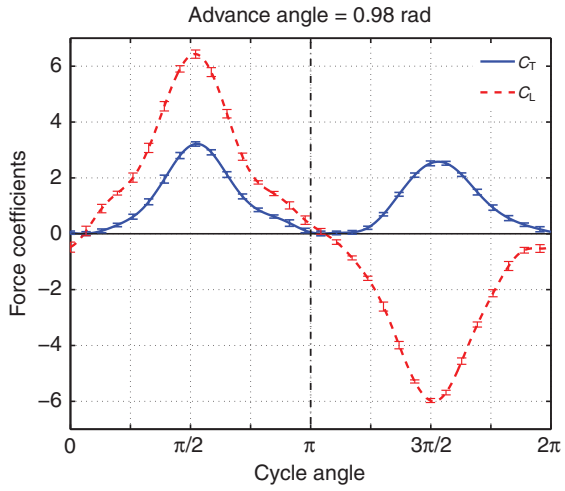

Fig. 6. Phase averaged thrust coefficient, C_T, and lift coefficient, C_L, for symmetric foil motion, with downstroke $\alpha_{max}=40$ deg., upstroke $\alpha_{max}=40$ deg., and Strouhal number $St=0.4$. Errors bars shown.

are generated by the symmetric foil kinematics, with equal sign (positive) thrust but opposite sign lift force produced during the downstroke and the upstroke, respectively, resulting in high mean thrust and zero mean lift. The forces exhibit a single peak in each half of the period; the peak occurs around phase angle $\pm\pi/2$.

The next step is to run an experiment with asymmetric kinematics but no in-line motion. We fix, then, $A_{X/Y}=0$ and calculate kinematics to yield the required transverse motion, and downstroke maximum angle of attack $\alpha_{max}=40$ deg., while the upstroke maximum angle of attack is $\alpha_{max}=0$ deg., at Strouhal number $St=0.40$. As seen in Fig. 7, the asymmetric foil kinematics provide positive mean thrust only during the downstroke; net drag is measured during the upstroke when fully feathered upstroke motion is employed. Also, the mean lift produced by the asymmetric foil kinematics is always positive, during both the downstroke and the upstroke. Setting the upstroke nominal angle of attack close to zero has resulted in the generation of relatively small but positive lift forces, which aid the upward motion of the foil during upstroke.

The multiple lift and thrust peaks observed during the upstroke are evidence of the memory effects in the wake of the vorticity shed during the downstroke; this is due to the fact that, although the linear (transverse) motion is identical during upstroke and downstroke, the angle of attack differs drastically. It is notable that over the downstroke both lift and thrust remain similar in value and close in shape to the forces measured for a symmetrically moving foil. Indeed, as seen in Fig. 6 and Fig. 7, the peak thrust and the peak lift occur at the same phase with comparable magnitude and direction, although the downstroke time trace has slight qualitative differences for these two cases. Feathering the upstroke has not fundamentally changed the force-generating mechanism in such a way as to dramatically reduce the available thrust on the downstroke, or either increase or decrease the lift forces perpendicular to the travel direction. The mean lift force obtained in asymmetric flapping, however, is usually undesirable for buoyant animals, except for maneuvering; in animal flight they could be used to provide steady lift.

Effect of in-line motion

A major driver for studying the in-line motion is the possibility of eliminating the mean lift force and reducing the memory effects from the wake, as well as enhancing thrust production. Indeed, an in-line motion which is timed to be negative during downstroke reduces the effective oncoming velocity and hence allows, for a constant angle of attack, a significant increase in the rotation of the foil, such that nearly the entire force is thrust; it also allows the foil during upstroke to move in the positive direction, moving away from wake memory effects, and hence avoiding negative lift peaks and drag forces. As a result, we systematically tested asymmetric flapping combined with in-line motion.

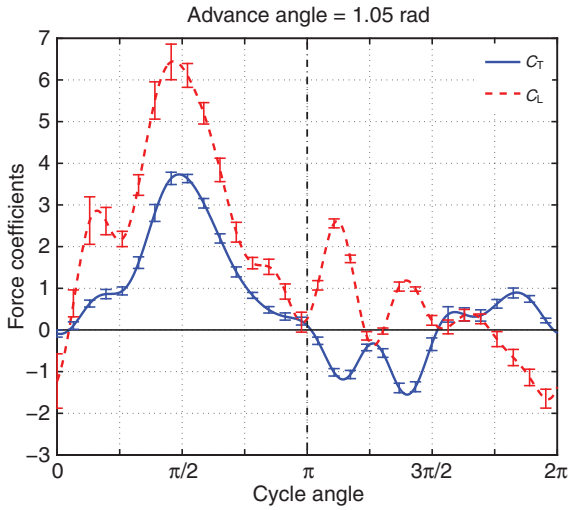

Fig. 7. Phase averaged thrust coefficient, C_T, and lift coefficient, C_L, for asymmetric foil motion, with downstroke $\alpha_{max}=40$ deg., upstroke $\alpha_{max}=0$ deg., and Strouhal number $St=0.4$, with no in-line motion relative to the steadily translating carriage. Errors bars shown.

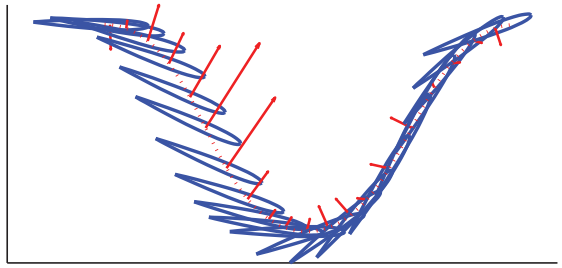

Fig. 8. Foil position with respect to fluid at regular intervals, where advance angle $\theta_{ADV}=0.385\pi$. Arrows represent recorded fluid force on foil.

Given that nearly the same total force is produced during the power stroke and the corresponding stroke of a symmetrically flapping foil, the rotation of the force to become nearly parallel to the direction of steady foil motion explains how the thrust is increased at the same time that the lift is decreased, as a result of the in-line motion. This is shown by Figs 8 and 9 for two different values of the advance angle, $\theta_{ADV}=0.385\pi$ (70 deg.) and $\theta_{ADV}=0.55\pi$ (100 deg.), respectively. As the advance angle increases, the foil moves increasingly backwards during the power stroke; its negative horizontal velocity reduces the oncoming velocity substantially and forces significant additional pitch rotation to preserve the angle of attack. The force vector rotates, likewise, producing substantial thrust and much reduced lift force, as seen with the vectors of forces in Figs 8 and 9.

The graphs of Fig. 10 provide a quantitative assessment of the impact of in-line motion, starting with no in-line motion (upper left, for advance angle 1.05 rad), which is the same as Fig. 8, and moving to higher values of the advance angle, corresponding to increasing in-line motion. It is clearly seen that during the downstroke, as advance angle increases, thrust force increases and lift force decreases. During the upstroke the effect of advance angle is much smaller; no attempt to optimize the motion during the upstroke was performed. Small variation of the angle of attack during upstroke could result in elimination of drag and reduction of unbalanced lift forces.

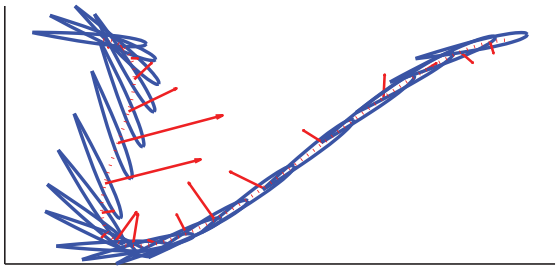

Fig. 9. Foil position with respect to fluid at regular intervals, where advance angle $\theta_{ADV}=0.55\pi$. Arrows represent recorded fluid force on foil.

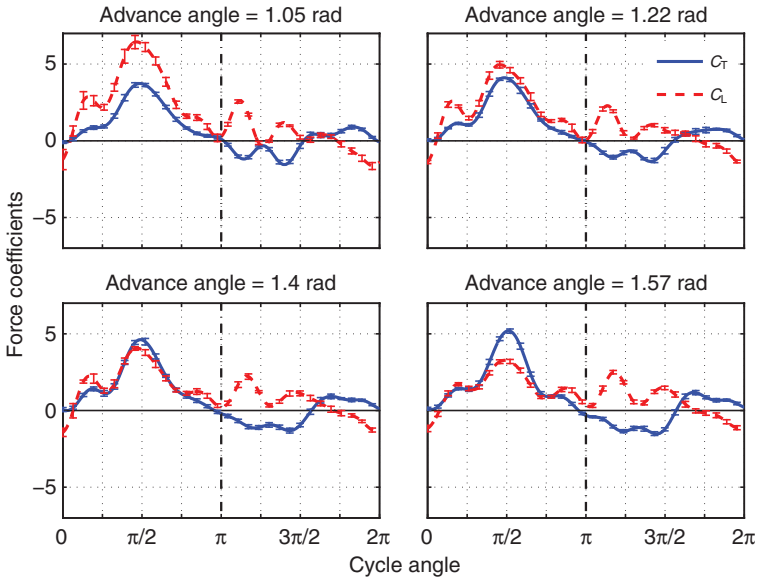

Fig. 10. Phase averaged thrust coefficient, C_T, and lift coefficient, C_L, for downstroke α_{max}=40 deg., Strouhal number St=0.4, for four cases with advance angles ranging from the minimum possible (no in-line motion) up to π/2, corresponding to no forward motion relative to the water in the center of the downstroke. Notice that thrust increases while lift decreases, as the advance angle increases. Error bars shown.

Measured mean lift and thrust coefficients are calculated as the average of the corresponding instantaneous forces over an entire cycle of motion:

$$\overline{C}_L = \frac{\frac{1}{T}\int_0^T \mathrm{L}(t)\,\mathrm{d}t}{\frac{1}{2}\rho U^2 S}\,, \tag{8}$$

$$\overline{C}_T = \frac{\frac{1}{T}\int_0^T \mathrm{T}(t)\,\mathrm{d}t}{\frac{1}{2}\rho U^2 S}\,. \tag{9}$$

As reference area S we use the (one-sided) area of the foil. It should be noted that while the area swept by the foil provides a better definition for the thrust coefficient in terms of propulsive performance, for practical purposes we chose, instead, the area of the foil so as to have a fixed area of reference for all experiments.

The mean lift and thrust results from the full set of experiments are shown in Figs 11 and 12, respectively, as a function of the advance angle and parameterized by the Strouhal number.

There are two trends that one anticipates (in the absence of in-line motion) as we move from symmetric flapping, where thrust is produced over the entire cycle and lift switches sign from the upstroke to the downstroke, to asymmetric flapping, where thrust is produced basically during the downstroke: an increased average lift and a reduced average thrust. Indeed, Figs 11 and 12 show this trend when the advance angle is comparable (i.e. no in-line motion in the asymmetric motion) between symmetric and asymmetric motion. For example, the drop in thrust moving from a high angle of attack upstroke to a fully feathered (zero angle of attack) upstroke, ranges from 42% at St=0.3 to 59% at St=0.6.

However, we see that as in-line motion increases in asymmetric motion, causing the advance angle to increase, the mean lift decreases substantially, even for high Strouhal numbers, and thrust increases to values close to (but slightly lower than), the symmetric motion values. In fact, for every Strouhal number tested (St=[0.2, 0.3, 0.4, 0.5, 0.6]) using asymmetric kinematics, the thrust increases monotonically with increasing advance angle, while the lift decreases monotonically; only for St=0.6 did we find a minimum value for the lift coefficient at very high advance angle. The thrust coefficient can increase substantially as advance angle increases, by as much as 225% between minimum and maximum advance angle, for St=0.6; coming close to the value for a symmetric foil (93% of the symmetric foil thrust for St=0.6).

The next question to address is the hydrodynamic efficiency (η) of the asymmetrically moving foil, defined as the useful work (average thrust force F multiplied by the steady forward velocity) divided by the work P expended by the foil on the fluid (work done by the actuators with the foil and motor inertial contribution removed), and calculated using the following equations:

$$P(t) = (\dot{x}(t),\dot{y}(t)) \cdot (F_x(t), F_y(t))\,, \tag{10}$$

$$\eta = \frac{U\int_0^T F_x(t)\,\mathrm{d}t}{\int_0^T P(t)\,\mathrm{d}t}\,, \tag{11}$$

where $(u, v)\cdot(X, Y)$ denotes the inner product of velocity and force. Note that the pitch motor power input is not accounted for, because it was found to be negligible.

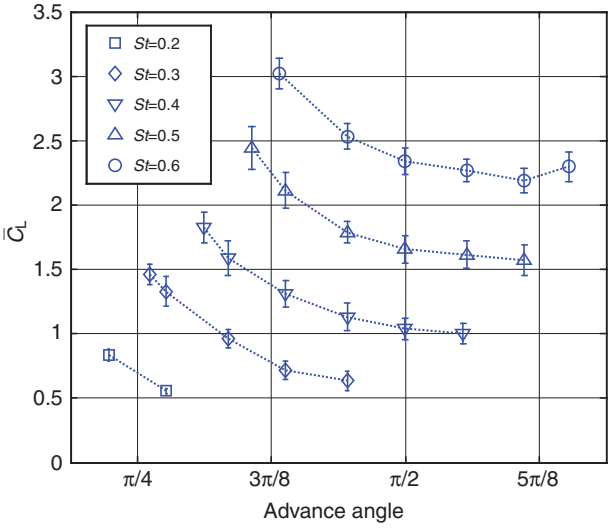

Fig. 11. Mean lift coefficient, $\overline{C}_L$, for asymmetric foil motion with downstroke α_{max}=40 deg., upstroke α_{max}=0 deg., for varying Strouhal number and advance angle. Error bars shown.

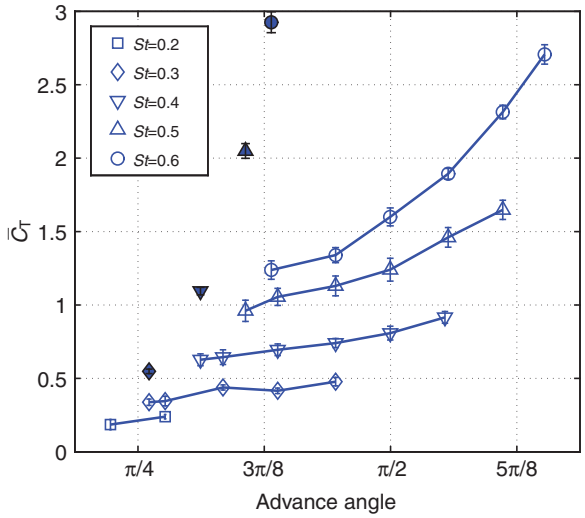

Fig. 12. Mean thrust coefficient, $\bar{C}_T$ for asymmetric foil motion with downstroke α_{max}=40 deg., upstroke α_{max}=0 deg., for varying Strouhal number and advance angle. Filled symbols indicate $\bar{C}_T$ for symmetric motions with no in-line motion, and upstroke α_{max}=40 deg. Error bars shown.

Fig. 13 provides the efficiency of the foil as a function of the advanced angle parameterized by the Strouhal number. The efficiency of the symmetrically moving foil is provided as well. As shown in the figure, the increasingly larger rotation of the force vector obtained during the downstroke as advance angle, θ_{ADV}, increases results not only in increased thrust production and decreased mean lift but also in a substantial increase in efficiency; up to a threshold value of the advance angle. The value of the advance angle where the maximum efficiency is obtained is only weakly dependent on Strouhal number, and seems to lie at around $\theta_{ADV} \approx 0.55\pi$ (100 deg.). The peak efficiency of the asymmetric motion is, in fact, higher than the efficiency of the symmetrically moving foil; for Strouhal numbers between 0.2 and 0.4 the asymmetric foil has significantly higher efficiency than symmetric foils.

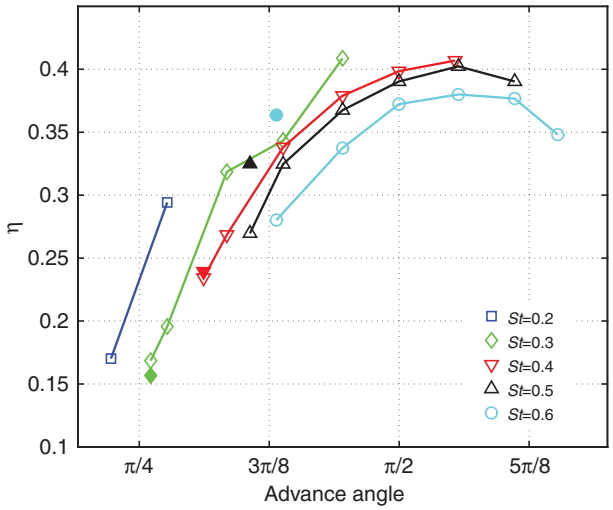

Fig. 13. Efficiency, η, of thrust production varying advance angle for foils with downstroke α_{max}=40 deg., upstroke α_{max}=0 deg., for all *St* numbers tested. Filled symbols indicate η for symmetric foil motions, with downstroke α_{max}=40 deg., upstroke α_{max}=40 deg., and no in-line motion, for each *St* number.

It should be noted that, certainly up to an advance angle of π/2, the addition of in-line motion does not change the basic thrust stroke from a lift-based to a drag-based mechanism, or rowing stroke. A direct comparison of the foil kinematics and dynamics (Figs 4, 5 and 8, 9, respectively) show clearly that the force is very nearly perpendicular to the relative velocity; this was found to be true in all the cases considered herein. Hence, despite substantial in-line motion the force production remains lift based.

DISCUSSION

Marine turtles use the two front semi-rigid, broad and flat flippers to propel their rigid bodies. Although turtles exhibit several other modes of motion, the focus of this study is on the propulsive power stroke, where the turtle uses the forelimbs to produce thrust, while the hindlimbs are used as rudders. These strokes employ a lift-based mechanism of generating thrust, as confirmed by the angle of attack measurements done by Davenport and colleagues (Davenport et al., 1984).

Although the turtle flippers rotate about a pivot point and also describe a complex three-dimensional motion, the simplified motion of the foils we used captures an essential feature of the turtle flipper motion that sets it apart from symmetrically flapping foils, *viz*. the effect of significant in-line motion. As a result, we expect the present results to shed light, at least qualitatively, on the principal mechanisms for optimizing asymmetric flipper motion.

The kinematics of sea turtles is explained in great detail by Wyneken (Wyneken, 1988). The motion of the forelimbs during the power stroke is angled at about 56 deg. from the horizontal, which translates to $A_{X/Y}$ of about 0.67, strong evidence that fore–aft motion of the type considered here is employed in the power strokes of sea turtles. Foil rotation was also observed during the downstroke, which serves to rotate the direction of the force, converting lift into thrust. The time taken for the upstroke motion was observed to be longer than the time taken during the downstroke even though the excursion distance was about the same. The slower upstroke is beneficial in reducing the unwanted drag and lift production during the upstroke, as they are proportional to the velocity squared and the velocity, respectively. The underlying muscle architecture of the sea turtle might also limit the availability of torque during upstroke, hence the slower velocity.

The findings by Wyneken are consistent with the foil experiment results herein. The slowing of the body that was observed to occur during the upstroke indicates that no significant net thrust was being produced during this part of the power stroke. The observation supports the hypothesis that the upstroke is a feathering (or recovery) stroke and the turtle does not produce thrust during upstroke. The conclusion that thrust is produced only during downstroke in optimized asymmetric flapping is consistent with the finding shown in Fig. 7. The observed substantial rotation of the turtle flipper during downstroke fits the description of foil motion after the introduction of in-line motion as well (Fig. 5). Direct observation of turtles in the New England Aquarium also confirmed the presence of in-line motion during the power stroke (Licht, 2008).

It should be noted that the optimized trajectory in the present experiments, consisting of downstream in-line motion during the power stroke and upstream motion during the feathering stroke, differ from the kinematics employed in animal flight. The in-line motion of wings in birds and bats is in the opposite direction from the optimal motion found herein; their motion is in the upstream direction during the power stroke and downstream during the upstroke (Tobalske and Dial, 1996; Tian et al., 2006). This difference is attributable to the significant lift force that must be generated for

flying animals – which is to be avoided for neutrally buoyant animals. Since the wings of bats and birds must produce substantial lift, they move in the upstream direction during the power stroke, to avoid the excessive rotation of the total fluid force, which would diminish lift; contrary to the optimal pattern for swimming turtles. Likewise, during the upstroke they move the wings downstream so as to take advantage of the proximity with previously shed vorticity and their suction forces (Lehmann, 2008) to produce lift even under feathering conditions, at the expense of producing some drag force. This is confirmed by the fact that as speed increases the axial motion is found to decrease (Tobalske and Dial, 1996), since the bird weight is fixed and the required lift coefficient decreases as speed decreases, while the thrust coefficient remains roughly constant. As with birds, Lindhe Norberg and Winter (Lindhe Norberg and Winter, 2006) find for bats that in their power stroke the angle with respect to the horizontal progressively increases from 45 deg. at 2.3 m s^{-1} to 77 deg. at 7.5 m s^{-1}; also, as a consequence, the Strouhal number gets closer to its optimal values for propulsion at highest speeds. Hedenström and colleagues (Hedenström et al., 2009) report similar observations for both birds and bats.

For animals employing both upstroke and downstroke as power strokes, we can also find similar traits: Borrell and colleagues (Borrell et al., 2005) studied the kinematics of *Clione antarctica*, a pteropod mollusc found in the Antarctic, one of the smallest aquatic flappers, swimming at low Reynolds numbers ($10<Re<100$). Although these pteropods use approximately similar downstrokes and upstrokes, each half-stroke consists of distinct power and recovery phases allowing them to utilize the same mechanism of transverse motion combined with an in-line motion in the direction of oncoming flow, as reported herein. The in-line to transverse motion ratio, expressed as the angle formed between these two vectors, β_{ps}, is found to increase with the forward speed, since this allows very efficient development of thrust while keeping the transverse force nearly constant. The value of β_{ps} increased nearly linearly with speed from a value of 18.5 to 31.7 deg. (Borrell et al., 2005). Finally, Walker and Westneat (Walker and Westneat, 1997) studied the pectoral fin locomotion in *Gomphosus varius*, a tropical coral reef fish which is 2.4% negatively buoyant. They remark that its fin is generating lift with large upward and small forward components during the downstroke whose motion is directed down and forward (as in birds), while during the upstroke (directed up and backwards) the fin is generating largely thrust.

CONCLUSIONS

The principal conclusion is that an asymmetric propulsive pattern, consisting of a power downstroke followed by a feathering upstroke, can be an efficient propulsive mode when combined with an in-line motion that is timed to move the foil downstream during the power stroke and upstream during the upstroke. In fact, this asymmetric propulsive mode, which is employed by sea turtles, can provide substantial thrust and high efficiency, comparable to those of a symmetrically flapping foil, while avoiding large steady lift forces.

The conclusions are based on experiments conducted at a Reynolds number of 13,000 on high aspect ratio rigid foils. The downstroke and upstroke maximum angles of attack were kept at 40 and 0 deg., respectively, while the upstroke and downstroke times were set to be equal. The transverse amplitude was constant, equal to 0.9 foil chords. These values are representative of moderately loaded foils. The two basic parameters that were varied systematically to conduct an optimization study were the Strouhal number, St, and the advance angle, θ_{ADV}; the latter was defined as the angle between the foil trajectory, at the middle of the downstroke, and the steady flow direction. For optimal values of the advance angle, around 0.55π (100 deg.), the average thrust is slightly lower but comparable to the thrust obtained by a symmetrically flapping foil, while the efficiency is as high, or higher. In addition, the average lift force is kept relatively small.

For nearly neutrally buoyant animals the results herein show that employing such a one-sided power stroke does not constitute a hydrodynamic handicap; the thrust and efficiency remain high and the total average lift force coefficient stays relatively small.

LIST OF ABBREVIATIONS AND SYMBOLS

A_X	amplitude of in-line motion
$A_{X/Y}$	amplitude ratio
A_Y	amplitude of in-line motion
c	chord length
C_L	lift coefficient
C_T	thrust coefficient
D	downstroke
f	frequency
F	force
h_0	amplitude of heave oscillation
pp	peak to peak
P	work
S	reference area
St	Strouhal number
T	duration
T_D	downstroke duration
T_U	upstroke duration
$T_{U/D}$	duration ratio T_U/T_D
U	upstroke
U	velocity
$\dot{x}$	velocity in the x-direction
$\dot{y}$	velocity in the y-direction
α	angle of attack
η	efficiency
θ	pitch angle
θ_{ADV}	advance angle
ω	frequency of oscillation in rad s^{-1}

ACKNOWLEDGEMENTS

We acknowledge with gratitude permission by the New England Aquarium to observe and film sea turtles and the expert assistance provided by the Aquarium's personnel. Financial support was provided by the MIT Sea Grant Program and CEROS.

REFERENCES

Anderson, J. M., Streitlien, K., Barrett, D. S. and Triantafyllou, M. S. (1998). Oscillating foils of high propulsive efficiency. *J. Fluid Mech.* **360**, 41-72.
Blake, R. W. (1980). The mechanics of labriform locomotion. II. An analysis of the recovery stroke and the overall fin-beat cycle propulsive efficiency in the angelfish. *J. Exp. Biol.* **85**, 337-342.
Blake, R. W. (2004). Fish functional design and swimming performance. *J. Fish Biol.* **65**, 1193-1222.
Blondeaux, P., Fornarelli, F., Guglielmini, L., Triantafyllou, M. S. and Verzicco, R. (2005). Numerical experiments on flapping foils mimicking fish-like locomotion. *Phys. Fluids* **17**, 113601-113612.
Borrell, B. J., Goldbogen, J. A. and Dudley, R. (2005). Aquatic wing flapping at low Reynolds numbers: swimming kinematics of the Antarctic pteropod, *Clione antarctica*. *J. Exp. Biol.* **208**, 2939-2949.
Buchholz, J. H. J. and Smits, A. J. (2006). On the evolution of the wake structure produced by a low-aspect-ratio pitching panel. *J. Fluid Mech.* **546**, 433-443.
Buchholz, J. H. J. and Smits, A. J. (2008). The wake structure and thrust performance of a rigid low-aspect-ratio pitching panel. *J. Fluid Mech.* **603**, 331-365.
Davenport, J., Munks, S. A. and Oxford, P. J. (1984). A comparison of the swimming of marine and freshwater turtles. *Proc. R. Soc. Lond.* B **220**, 447-475.
Dickinson, M. H., Lehmann, F. O. and Sane, S. P. (1999). Wing rotation and the basis of insect flight. *Science* **284**, 1954-1960.
Dong, H., Mittal, R. and Najjar, F. M. (2006). Wake topology and hydrodynamic performance of low-aspect-ratio flapping foils. *J. Fluid Mech.* **566**, 309-343.
Ellington, C. P. (1999). The novel aerodynamics of insect flight: application to micro-air vehicles. *J. Exp. Biol.* **202**, 3439-3448.
Hedenström, A., Johansson, L. C. and Spedding, G. R. (2009). Bird or bat: comparing airframe design and flight performance. *Bioinsp. Biomim.* **4**, 015001 (1-13).

Hover, F. S., Haugsdal, O. and Triantafyllou, M. S. (2004). Control of angle of attack profiles in flapping foil propulsion. *J. Fluids Struct.* **19**, 37-47.
Koochesfahani, M. M. (1989). Vortical patterns in the wake of an oscillating airfoil. *AIAA J.* **27**, 1200-1205.
Lauder, G. and Jayne, B. (1996). Pectoral fin locomotion in fishes: Testing drag-based models using three-dimensional kinematics. *Am. Zool.* **36**, 567-581.
Lauder, G. V., Madden, P., Mittal, R., Dong, H. and Bozkurttas, M. (2006). Locomotion with flexible propulsors I: Experimental analysis of pectoral fin swimming in sunfish. *Bioinsp. Biomim.* **1**, S25-S34.
Lehmann, F. O. (2008). When wings touch wakes: understanding locomotor force control by wakewing interference in insect wings. *J. Exp. Biol.* **211**, 224-233.
Licht, S. (2008). *Biomimetic Oscillating Foil Propulsion To Enchance Underwater Vehicle Agility And Maneuverability.* PhD dissertation. Massachusetts Institute of Technology.
Licht, S., Polidoro, V., Flores, M., Hover, F. and Triantafyllou, M. S. (2004). Design and projected performance of a flapping foil auv. *IEEE J. Oceanic Engineering* **29**, 786-794.
Lindhe Norberg, U. M. and Winter, Y. (2006). Wing beat kinematics of a nectar-feeding bat, *Glossophaga soricina*, flying at different flight speeds and Strouhal numbers. *J. Exp. Biol.* **209**, 3887-3897.
Lovvorn, J. R. (2001). Upstroke thrust, drag effects, and stroke-glide cycles in wing-propelled swimming by birds. *Am. Zool.* **41**, 154-165.
Ramamurti, R., Sandberg, W. C., Lohner, R. and Walker, J. A. (2002). Fluid dynamics of flapping aquatic flight in the bird Wrasse: three dimensional unsteady computations with fin deformation. *J. Exp. Biol.* **205**, 2997-3008.
Read, D. A., Hover, F. S. and Triantafyllou, M. S. (2003). Forces on oscillating foils for propulsion and maneuvering. *J. Fluid Struct.* **17**, 163-183.
Rohr, J. J. and Fish, F. E. (2004). Strouhal numbers and optimization of swimming by odontocete cetaceans. *J. Exp. Biol.* **207**, 1633-1642.
Shyy, W. and Liu, H. (2007). Flapping wings and aerodynamic lift: the role of leading-edge vortices. *AIAA J.* **45**, 2817-2819.
Suzuki, H., Kato, N. and Suzumori, K. (2008). Load characteristics of mechanical pectoral fin. *Exp. Fluids* **44**, 759-771.
Taylor, G. K., Nudds, R. L. and Thomas, A. L. R. (2003). Flying and swimming animals cruise at a strouhal number tuned for high power efficiency. *Nature* **425**, 07711.
Techet, A. H., Lim, K. L., Hover, F. S. and Triantafylou, M. S. (2005). Hydrodynamic performance of a biologically inspired 3D flapping foil. In *Proceedings Of The 14th International Symposium On Unmanned Untethered Submersible Technology*, pp. 463-469. Durham, New Hampshire; Autonomous Undersea Systems Institute.
Tian, X., Iriarte-Diaz, J., Middleton, K., Galvao, R., Israeli, E., Roemer, A., Sullivan, A., Song, A., Swartz, S. and Breuer, K. (2006). Direct measurements of the kinematics and dynamics of bat flight. *Bioinsp. Biomim.* **1**, S10-S18.
Tobalske, B. W. and Dial, K. P. (1996). Flight kinematics of black-billed magpies and pigeons over a wide range of speeds. *J. Exp. Biol.* **199**, 263-280.
Triantafyllou, M. S., Triantafyllou, G. S. and Gopalkrishnan, R. (1991). Wake mechanics for thrust generation in oscillating foils. *Phys. Fluids A* **3**, 2835-2837.
Triantafyllou, M. S., Hover, F. S., Techet, A. H. and Yue, D. K. P. (2005). Review of hydrodynamic scaling laws in aquatic locomotion and fish-like swimming. *App. Mech. Rev.* **58**, 226-237.
Videler, J. and Kamermans, P. (1985). Differences between upstroke and downstroke in swimming dolphins. *J. Exp. Biol.* **119**, 265-274.
von Ellenrieder, K. D., Parker, K. and Soria, J. (2003). Flow structures behind a heaving and pitching finite-span wing. *J. Fluid Mech.* **490**, 129-138.
Walker, J. A. and Westneat, M. W. (1997). Labriform propulsion in fishes: kinematics of flapping aquatic flight in the bird wrasse, *Gomphosus varius* (*labridae*). *J. Exp. Biol.* **200**, 1549-1569.
Wolfe, M., Licht, S., Hover, F. S. and Triantafyllou, M. S. (2006). Open loop performance of 'Finnegan', the biomimetic flapping foil AUV. In *Proceedings Of The Sixteenth (2006) International Offshore And Polar Engineering Conference*, vol. II, pp. 247-253. Cupertino, CA: International Society of Offshore and Polar Engineers (ISOPE).
Wyneken, J. (1988). *Comparative And Functional Considerations Of Locomotion In Turtles.* PhD dissertation. University of Illinois at Urbana-Champaign, Department of Ecology, Ethology and Evolution.